Journal of Hydrology: Regional Studies 58 (2025) 102224

Contents lists available at ScienceDirect

Journal of Hydrology: Regional Studies

journal homepage: www.elsevier.com/locate/ejrh

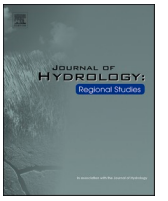

Estimation of evaporation in Andalusian reservoirs: Proposal of an index for the assessment and classification of dams

Santiago García-López [a,c], Marcia Salazar-Rojas [b,*], Mercedes Vélez-Nicolás [a,c], Jorge. M.G.P. Isidoro [d,e], Verónica Ruiz-Ortiz [b]

[a] Geoscience Research Group, RNM 373, Faculty of Marine and Environmental Sciences, Campus Río San Pedro, University of Cadiz, Puerto Real, Spain
[b] Geoscience Research Group, RNM 373, Algeciras School of Engineering and Technology, Campus Bay of Algeciras, University of Cadiz, Algeciras, Spain
[c] INMAR - Institute for Marine Research, Campus Río San Pedro, University of Cadiz, Puerto Real, Spain
[d] Department of Civil Engineering, Institute of Engineering, University of Algarve, Campus da Penha, Faro, Portugal
[e] CIMA - Centre for Marine and Environmental Research / ARNET - Aquatic Research NETwork, Campus de Gambelas, Faro, Portugal

ARTICLE INFO

Keywords:
Reservoir Evaporation
Large Dams
Classification Index
Andalusian Reservoirs, Reservoir Efficiency

ABSTRACT

Study region: This study focuses on Andalusia (Southern Spain), a mediterranean region of 87,270 km^2. Andalusia experiences significant water stress, making effective water management crucial.
Study focus: Evaporation is a key element of the water budget, particularly in arid and semi-arid climates, where losses from reservoirs represent a significant fraction of the volume annually regulated and compromise the efficiency of these infrastructures. This study aims to (i) estimate the annual volume of water evaporated from large dams ($>$ 5 hm^3) in Andalusia and (ii) propose an index to classify reservoirs based on evaporative losses.
New hydrological insights for the region: Data from 76 large dams in Andalusia, including their descriptive characteristics, morphometric details, and hydrological information, were retrieved from institutional sources. The monthly average flooded area was calculated from the Area-Volume-Elevation (AVE) curve, while monthly average evaporation rate was calculated through the FAO Penman-Monteith equation using meteorological data. The combination of both variables has allowed to estimate the mean monthly volume of water evaporated in each reservoir. Results were validated with isotopic content (^{18}O and ^{2}H) from selected reservoirs. The annual average volume evaporated from Andalusian reservoirs was estimated at 547 hm^3/year (8.0 % of the inflows). Evaporative losses represent 1.1 % of inflows in the most efficient reservoirs, while in others, losses exceed 30 %, reaching 54 % in the most extreme case.

1. Introduction

Evaporation is a fundamental element in the hydrological cycle that can induce large water losses in surface water bodies and affect other environmental systems, including soils, depending on their level of moisture, and very shallow aquifers. Human intervention in

* Corresponding author.
E-mail addresses: santiago.garcia@uca.es (S. García-López), marcia.salazar@uca.es (M. Salazar-Rojas), mercedes.velez@uca.es (M. Vélez-Nicolás), jisidoro@ualg.pt (Jorge.M.G.P. Isidoro), veronica.ruiz@uca.es (V. Ruiz-Ortiz).

https://doi.org/10.1016/j.ejrh.2025.102224
Received 10 October 2024; Received in revised form 21 December 2024; Accepted 31 January 2025
Available online 7 February 2025

the hydrological cycle through the construction of regulation infrastructures, such as dams, modifies the water balance of the region and enhance the loss of water resources to the atmosphere due to evaporation. The evaporative losses attributable to these hydraulic infrastructures can be estimated as the difference between the evaporation from the flooded surface and the evapotranspiration that might naturally take place on that land surface, if the infrastructure had not been built. According to (Témez, 2007), in humid climates with densely vegetated areas, the actual evapotranspiration (AET) is very close to the potential evapotranspiration (PET) throughout the year, because there is enough water available in the soil to satisfy the evaporative demand of the atmosphere. This is why the negative impacts derived from the construction of reservoirs in terms of evaporation losses are less severe. On the contrary, in arid and semi-arid climates, the availability of water in the soil during most of the year is very low, sometimes practically zero. This makes AET significantly lower than PET. In this case, flooding the valley leads to a significant increase in water availability, compared to the previous situation, so that the evaporative demand of the atmosphere can be completely satisfied, consequently increasing evaporative water losses in the reservoir area.

In the Mediterranean region, which is affected by high or extremely high-water stress, reservoirs are strategic elements for hydrological planning and meeting irrigation, industrial and urban demands, as well as for the generation of energy. Given the importance of reservoirs in such climatic contexts, assessing the impact of reservoirs on evaporative processes and the associated loss of water resources becomes a priority. To minimize infrastructure inefficiencies, evaporation should receive special attention from the initial stages of reservoir design and throughout the subsequent operation, management, and resource allocation stages. However, the magnitude of these evaporative losses is usually underestimated owing to the practical and logistical challenges and large uncertainties in its quantification (Friedrich et al., 2018). Several factors affect evaporative losses; some are intrinsic to the infrastructure (*e.g.*, morphometry and thermal regime of the reservoir), and others extrinsic such as climate (*e.g.*, air/water temperature, humidity, wind speed, solar radiation), physiography or climate change (Da Costa et al., 2021; Ruiz-Ortiz et al., 2021). Besides, the physical processes related to evaporation are highly non-linear (Kisi, 2007), hindering its estimation. For instance, evaporation in deep reservoirs is higher during winter and decreases in summer, compared to what was expected, contrarily to shallow reservoirs. These differences are caused by the thermal regulation exerted by the deep-water layers, which can store large amounts of heat; during spring and summer, the intense solar radiation is slowly transferred in the form of heat to deeper layers with some lag, due to the high specific heat of water. Subsequently, in the cold months, the stored heat returns to the atmosphere partly through evaporation. These phenomena are enhanced by thermal inversion processes in the water body, which boost internal heat transfer mechanisms such as convection currents.

The aim of this study is to carry out a preliminary assessment of the annual evaporative losses from 76 large dams (> 5 hm^3) of Andalusia (southern Spain), a mediterranean region characterized by a highly variable rainfall regime, recurrent droughts, and particularly vulnerable to water resource scarcity owing to its socioeconomic characteristics. The results have been compared with the isotopic content (^{18}O and ^{2}H) of some of the reservoirs under analysis. In addition, we propose a combined index based on several morphometrical and hydrological variables for the classification of reservoirs according to the magnitude of these losses. The information generated is intended to serve as a useful reference for water resources management as well as for future reservoir operation and design in arid and semi-arid regions.

2. Background

As seen previously, evaporation is influenced by various factors intrinsic to the reservoir and extrinsic factors such as climate, physiography, and climate change. The magnitude of evaporation can vary significantly across climatic zones and reservoir characteristics. For instance, evaporation from deep reservoirs is typically higher in winter and lower in summer compared to shallow reservoirs. These seasonal differences arise from the thermal regulation exerted by deep-water layers, where intense solar radiation is gradually transferred to deeper layers during spring and summer, with heat released in colder months.

To address these challenges, several methods have been developed for the quantification of evaporation in reservoirs. These methods can be grouped into five main categories: 1) Direct measurements 2) Water budget estimation, 3) Energy budget, 4) Mass transfer methods and 5) Semiempirical equations.

1. Direct measurements usually rely on different types of evaporation pans/evaporimeters or on the application of Eddy covariance techniques. Regarding the first, among the many different types of evaporation pans available, the most used is the class A evaporimeter due to its low cost and simplicity (Alazard et al., 2015). Evaporation pans usually require the application of reducing coefficients to minimize the “oasis effect” caused by the advective heat, which is variable depending on the location of the tank (Témez, 2007). In this regard, several authors (Lowe et al., 2009; Alvarez et al., 2007; Martínez Álvarez et al., 2004) have estimated reduction coefficients for different regions considering different factors, such as the dimensions of the reservoir, water column stratification, the presence of aquatic plants, temperature, relative humidity, wind speed, turbidity, and salinity. These coefficients vary throughout the year and should be calculated for each month individually. The uncertainty in the estimations from evaporation pans stem from the correction coefficients, the spatial transposition factor, the lack of maintenance and cleaning of the devices, and from unfavorable weather conditions that might hinder correct measurements (Craig et al., 2005; Gökbulak and Özhan, 2006; Lowe et al., 2009). Such uncertainty, however, decreases significantly if the measuring device is located near the reservoir. Because of this, some authors even suggest placing floating evaporimeters on water surface to better simulate the evaporation conditions. With respect to the Eddy Covariance method, it is based on the quantification of surface fluxes from in-situ measurements of vertical wind speed, air temperature, and specific humidity using advanced sensors (*e.g.*, sonic anemometers and thermometers and infrared sensors). This methodology ensures accurate estimations of evaporation, but its application is usually

limited by its complexity and high costs of the equipment (Miranda Rodrigues et al., 2020, Althoff et al., 2019). Another drawback of the Eddy Covariance method is the high frequency attenuation caused by the relatively slow response time of the sensors, which is improving notably with the latest technological advances.

2. Water budget methods are based on the principle of mass conservation, which stipulates that variations in the stored volume are the result of the difference between the outputs and inputs into the system. Stored water and water flows must be measured, although some variables of the balance are considered negligible. In this case, the uncertainty of the method is conditioned by the accuracy in the estimation of the different elements of the water balance. Since precipitation inputs and evaporation and infiltration outputs are

Table 1
Summary of relevant studies on evaporation from reservoirs, lakes, and ponds carried out in arid and semi-arid areas.

Autor	Region	Reservoir, lakes, or ponds studied	Annual evaporative loss (hm^3)	Methods	Limitations
(Martínez Álvarez et al., 2004)	Campo de Cartagena (Spain)	3490 agricultural ponds	8	Pan evaporation data and pan coefficients.	Pan evaporation data uncertainty.
(Gökbulak and Özhan, 2006)	Turkey	129 lakes and 223 reservoirs	6800	Pan evaporation data and pan coefficients.	Data gaps during winter season.
(López Moreno, 2008)	N Spain	7 reservoirs	67	Penman equation.	The adoption/consideration of constant wind speed due to lack of reliable records may cause underestimation.
(Martínez-Granados et al., 2011)	SE Spain	15,000 agricultural ponds and 14 large reservoirs	82	Class-A pan evaporation data and pan coefficients.	Maintenance problems or sensor failures that negatively impact data reliability.
(Wurbs and Ayala, 2014)	Texas (USA)	3415 reservoirs	7530	Pan evaporation data and pan coefficients.	Spatial extrapolation of pan evaporation data. Lake/pan coefficients. (Seasonally coef. more accurate than annual coef.).
(Zhang et al., 2017)	Texas (USA)	200 major reservoirs	8000	Pan evaporation data and pan coefficients.	Pan evaporation exceeds lake evaporation in spring and summer, while lake evaporation surpasses pan evaporation in fall and winter.
(Zhao and Gao, 2019)	USA	721 reservoirs	33,730	Penman equation.	Formulation of the wind function in the Penman equation.
(El and Mehanna, 2019)	Ethiopia & Sudan	10 reservoir and water body	9130	Modified analytical evaporation equations.	Lack of measured data. No climate variability impacts on atmospheric temperature, precipitation, nor evaporation rates are considered in this manuscript.
(Fuentes et al., 2020)	New South Wales, Australia	Namoi basin	202	FAO Penman-Monteith equation.	Limitations of Landsat imagery. Assumptions in the reference datasets, such as the constant wind speed, may introduce errors in evaporation estimations.
(Tian et al., 2021)	China	916 large reservoirs	14,020	Penman equation.	Ice sublimation. The meteorological data used to calculate evaporation has uncertainty.
(Tian et al., 2022)	Global	7242 reservoirs	339,800	Penman equation.	Ice sublimation. The meteorological data used to calculate evaporation has uncertainty.
(El Bilali et al., 2022)	Morocco.	49 small reservoirs	1.5	Pan evaporation data and pan coefficients.	Reduced fluctuations in reservoir stage led to large uncertainties in the estimation of reservoir areas.
(Xia et al., 2022)	NW China	167 reservoirs	492	Penman equation.	The measurement of uncertainty, climatic factor uncertainties.
(Li et al., 2023)	Hubei, China	Three Gorges Reservoir	565	Pan evaporation data and pan coefficients.	Daily pan evaporation data uncertainty.
(Aminzadeh et al., 2024)	Italy, Spain, and Portugal	1800 agricultural Ponds	72	Energy budget for quantifying surface fluxes and vertical temperature profiles.	Estimations of reservoir surface area depends on Global Surface Water data accuracy. Lacking detailed characteristics may affect evaporation rates.
(Li et al., 2024)	Hubei, China	Danjiangkou Reservoir.	595	Remote-sensing data, and the Generalized Complementary Relationship method (GCR).	Lack of measured values for comparison. Data resolution impact.
(Nevermann et al., 2024)	Water-stressed regions worlwide	10 large reservoirs	26,500	1D physically-based energy balance model.	Limited by its data requirements (e.g., high-resolution meteorological and bathymetric inputs) and computational complexity, making it less suitable for large-scale applications.

conditioned by the surface area of the reservoir, miscalculation of this variable can lead to the overestimation or underestimation in the quantification of those terms (Fowe et al., 2015).

3. The method of energy balance, also known as Bowen's method (BREB), is a relatively simple and practical technique for the direct estimation of the latent heat flux based on the energy conservation law. It requires measuring the temperature and vapor pressure gradients in the air, to calculate the Bowen ratio and the sensible and latent heat fluxes. To apply this method and determine the input parameters it is necessary to monitor the temperature profile in the reservoir, a demanding task in terms of instrumentation and personnel. In any case, the Bowen method is usually a benchmark for comparison with other methods due to its accuracy (Majidi et al., 2015; Rosenberry et al., 2007; Winter et al., 2003) and, despite its limitations, several authors recommend its use for long-term monitoring of evaporative processes (Gianniou and Antonopoulos, 2007; Pérez and Castellví, 2002; Winter et al., 2003). Among the constraints of the method are the reduction in accuracy when applied in deep water bodies, as well as the underestimation of evaporation during periods of high-speed winds (Bozorgi et al., 2020; Finch and Hall, 2001).

   Nevermann et al. (2024) and Zhao et al. (2020) aim to enhance evaporation estimates through advanced modeling of water temperature and energy balance. Nevermann et al. (2024) uses a physically based 1D energy balance model to solve for radiative flux and thermal diffusion, directly calculating evaporation based on vapor pressure differences and atmospheric conditions, Zhao et al. (2020) on the other hand, employs the Lake Temperature and Evaporation Model (LTEM), integrating MODIS water surface temperature data to simulate vertical temperature profiles, calculate heat storage, and improve seasonal evaporation accuracy, particularly for deep lakes.
4. Mass transfer methods are based on Dalton's Law and allow to estimate in a convenient and accurate way the evaporation from free water surfaces. In this case, the input variables are wind speed and the difference of vapor pressure between actual and saturated vapor pressure (El-Mahdy et al., 2021). One of the main disadvantaged of the method according to Singh and Xu (1997) is that its application is restricted to the specific area where the data was obtained originally, since the input parameters cannot be extrapolated to other locations, even with similar climatic conditions. Owing to the methodological inconsistency in the measurement of temperature and wind, there are many versions of the original equation that differ in the input parameters, hindering standardization and comparison between studies. These inconsistencies arise from differences in measurement heights, and data collection procedures (Singh and Xu, 1997). Other errors in the calculation of evaporation through mass transfer are related to inaccuracies in the estimation of the transfer coefficient, which is a function of wind speed (Finch and Hall, 2001).
5. The Penman equation (Penman, 1948) and its variants such as the Priestley-Taylor equation (Priestley and Taylor, 1972) or the FAO-Penman-Monteith (Allen et al., 2006) are robust and reliable methods, but their application is sometimes limited by the large number of meteorological variables required. As it will be explained subsequently, the Penman formula and its variants are widely used in reservoirs with different geometries and meteorological conditions, owing to their physical basis and because they combine the mass transfer and the energy balance methods. In the case of very deep and stratified water bodies, and to avoid overestimation in the calculation of evaporation, it is convenient to consider thermal storage, which can be estimated through the equilibrium temperature (Tian et al., 2021; Finch and Hall, 2001; Martínez Álvarez et al., 2004). Also, the input variables needed to feed the equation may increase uncertainty if there are no continuous and reliable records of wind speed in the area (López Moreno, 2008).

In the last decades, satellite-borne and more recently UAV (Unmanned Aerial Vehicle) remote sensing are emerging as promising tools for the study of evaporative processes (Guerschman et al., 2009; Martínez Álvarez et al., 2004) and several authors affirm that the integrated use of multiple remote sensing data sources is the future for improving global and local water monitoring (Huang et al., 2018; Sogno et al., 2022; Yang et al., 2022).

Several authors have assessed the accuracy, sensitivity, and simplicity of the above-mentioned methods to determine which is the most suitable for quantifying evaporation. For instance, Majidi et al. (2015) applied the energy budget approach, as well as 18 other methods, to estimate evaporation from a reservoir in NE Iran, concluding that the methods based on air temperature or its combination with solar radiation (*e.g.*, Jensen-Haise and Makkink methods) performed better. Rosenberry et al. (2007) compared 15 evaporation estimation methods over a small mountain reservoir in the northeastern USA. Gorjizade et al. (2014) evaluated evaporation in a reservoir located in a semi-arid region of Iran using 8 different methods and report that the best results were obtained by the Priestley-Taylor, de Bruin-Keijman, and Penman. However, given the large number of input variables required, these methods may not be cost-effective, in which case other methods such as Thornthwaite or Papadakis would be more suitable or feasible.

Several studies on the quantification of evaporation in reservoirs and lakes, and ponds at different scales can be found in the scientific literature. Table 1 summarises some relevant experiences developed in arid and semi-arid environments.

Given the magnitude of evaporation in many reservoirs, a plethora of biological, physical, and chemical methods have been devised to reduce water losses from these infrastructures. Biological methods include the maintenance of floating aquatic plants and planting tree or shrub windbreaks, alternatives that can reduce evaporation by up to 47 % and 6 %, respectively (Deepika et al., 2020; Youssef and Khodzinskaya, 2019). Chemical methods consist of the addition of evaporation inhibitors such as fatty alcohols (*e.g.*, Cetyl/Stearyl alcohol) to the reservoir to create a film that hinders evaporation, achieving reductions up to 30 % (Youssef and Khodzinskaya, 2019). However, the serious disadvantage of the chemical methods is the addition of artificial substances to the natural environment, which can cause problems from an environmental and consumptive point of view. Finally, physical methods are in general very efficient, reducing evaporation by up to 40 %, although investment and maintenance costs are quite high (Martinez-Alvarez et al., 2010; Shalaby et al., 2021). These physical methods comprise alternatives such as (i) Continuous or modular floating structures that reduce evaporation by up to 95 % (Youssef and Khodzinskaya, 2019, Aminzadeh et al., 2018; Assouline et al., 2011; Han et al., 2020; Han et al., 2019; Rezazadeh et al., 2020; Shalaby et al., 2021); (ii) Injection of air bubbles to break vertical stratification, achieving reductions in evaporation up to 6 % (Helfer et al., 2011), and (iii) Floating photovoltaic covers. This last method has sparked great interest for its

twofold function, significantly reducing evaporation (33–50 %) while generating renewable energy (El Bilali et al., 2022; Miranda Rodrigues et al., 2020), with some additional advantages, like saving land area, improving power generation, and the ability to combine it with hydroelectric power generation to improve economic efficiency (Huang et al., 2023).

3. Study area

Andalusia, where the reservoirs under analysis are located, is a region of the southernmost part of the Iberian Peninsula. With an area of 87,270 km^2, it accounts for 17 % of the Spanish territory. From a physiographical context, three domains can be identified from north to south: Sierra Morena, the Guadalquivir Valley, and the Baetic Cordillera, which registers the highest altitudes of the peninsular territory (3481 m.a.s.l.). Concretely, 45 % of the Andalusian territory displays altitudes over 500 m, which correspond to the reliefs of the Baetic Cordillera, 25.5 % ranges between 200 and 500 m, while only 29.5 % present altitudes below 200 m, coinciding with the Guadalquivir Valley depression and some coastal areas.

Six climatic subcategories have been described in the region. The most widespread is the "Mediterranean with dry, hot summers and soft winters" (Category "Csa" according to the Köppen–Geiger classification (Köppen, 1936)). The other five climate sub-types occupy smaller extensions of the Andalusian geography. These range from semi-tropical in the Southeastern and arid climates in the East (sub-types Bsk, Bwk, Bsh and Bwh), to continental climates with warm and cool winters in the hilly areas (sub-type Dsh). Rainfall displays a strong interannual irregularity and concentrates mainly on the autumn and winter months, with practically no precipitation between June and September. The average annual precipitation is close to 500 mm/year, ranging between 200 and 1100 mm/year with the local exception of Sierra de Grazalema, near to the Strait of Gibraltar, where rainfall exceeds 2000 mm/year. Potential evapotranspiration (PET) ranges between 300 mm on the higher summits of the Baetic Systems to more than 1000 mm in areas of the Guadalquivir Valley. The average annual temperature is approximately 16 ºC (1998–2007), showing a marked orographic dependence. Furthermore, the region is under high insolation and solar radiation, with averages of 2700 h/year and 5 kw/h/m^2 respectively, due to its subtropical latitude, the predominance of anticyclonic conditions, and the high angle of solar incidence. A detailed description of the climatology of Andalusia can be found at Junta de Andalucía (2022a)

Regarding hydrography, Andalusia is divided into six Hydrographic Demarcations (Fig. 1). The most extensive is the Guadalquivir River basin, which extends over the territory from E to W. The rest of the demarcations are smaller basins that drain towards the Mediterranean Sea or the Atlantic Ocean, the latter constituting several intra-community basins (Andalusian Mediterranean Basins, Guadalete-Barbate Basin, and Tinto, Odiel and Piedras Basin). Furthermore, the Andalusian territory also includes a part of two contiguous hydrographic basins, the Guadiana basin and the Segura basin (Table 2).

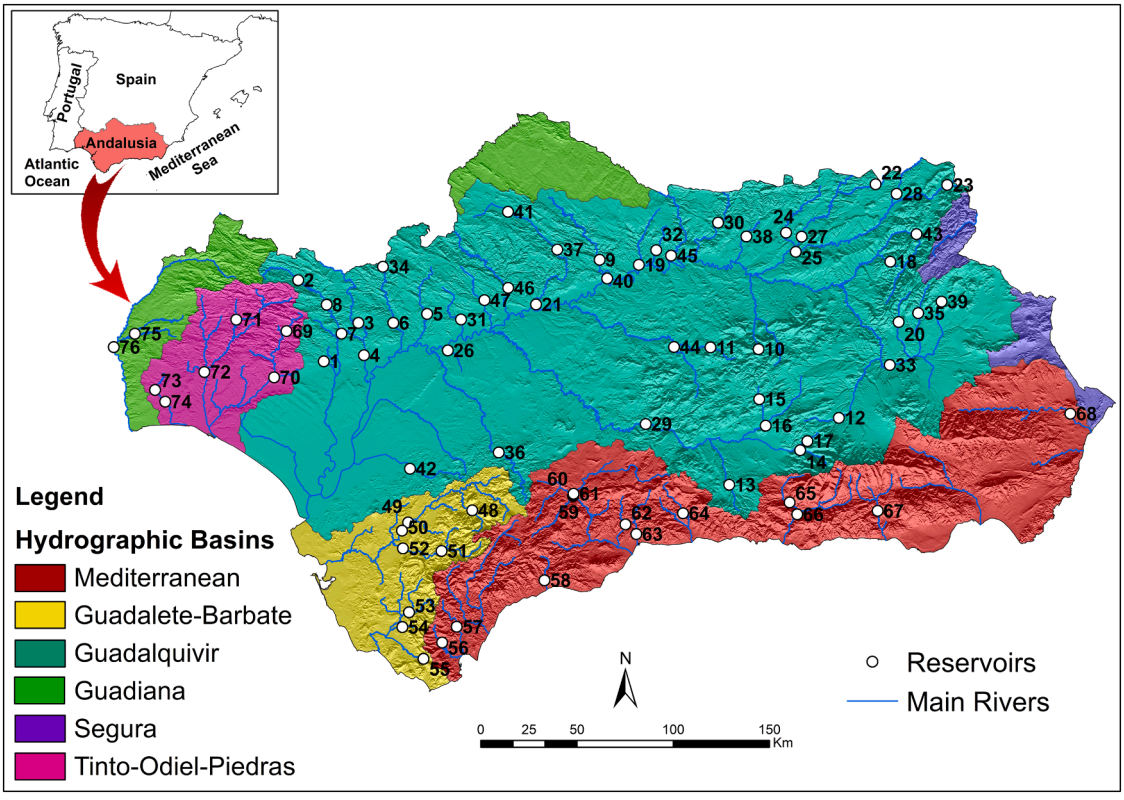

Fig. 1. Hydrographic Demarcations and location of the 76 reservoirs considered in this study (Modified from CMAOT, 2014).

Population in Andalusia reached 8,472,407 inhabitants in 2021 (INE, 2022), approximately 18 % of the Spanish population, displaying a notable rising demographic trend over the past five years. The total annual water demand in Andalusia is estimated at 5425 hm^3/year. Agriculture relies on large volumes of water for irrigation during the dry season, consuming about 4231 hm^3/year, representing 78 % of water resources to supply the large cropland extensions in the region. Moreover, most of the current irrigation systems are still supplied with surface water through open channels with the consequent evaporative losses. Urban supply is the second consumer of water resources (717 hm^3, representing 13.2 % of the total) (Junta de Andalucía, 2022b). The water resources used to meet these demands come from 80 reservoirs and more than 100 aquifers.

4. Data and methods

Our methodological workflow, comprising several stages (Fig. 2), proceeds as follows:

The first stage of this research consisted of compiling information on all the reservoirs with a capacity over 5 hm^3 in Andalusia (a total of 76 reservoirs) and complementary meteorological information. The information sources used were: (1) Spanish Dam Inventory (Ministerio de Agricultura, Pesca, Alimentación y Medio Ambiente, 2018), (2) Gauging Yearbooks (CEDEX, 2018), (3) The "Exploitation Systems" annex of each basin's Hydrological Plan for the period 2022–27, and (4) Meteorological data from the Agroclimatic Information Network of Andalusia (RIA). This network is managed by IFAPA (Agrarian and Fisheries Research and Training Institute-Water department of the Andalusian Regional government).

Source (1) was used to obtain the following information on each reservoir: location, construction year, maximum normal water level, height from foundation, crest length, dam body volume, type of construction, basin area, average annual contribution (project estimation), and reservoir capacity and maximum flooded area at maximum normal level. The dams analyzed in this study comprise a wide range of heights from foundations, between 9 and 156 m, with maximum storage capacities between 5 and 981 hm^3, and different construction typologies (embankment: 44.1 %, gravity: 38.1 %, arch-gravity: 9.5 %, double-curvature arch dam 7.1 %, buttress 1.2 %). The maximum storage capacity of this group of 76 large dams is 12,199 hm^3 (which represents approximately 28 % of the annual average volume of precipitation over Andalusia), with a flooded area of 608.6 km^2.

Source (2) was used to acquire data on the operation of each reservoir from its commissioning until 2018. The years after 2018 were not considered in the present study due to the persistent drought suffered in the region in subsequent years, which could bias the results, especially in those reservoirs recently commissioned. Specifically, the following aspects have been considered: period and number of years in which the infrastructure has been operating, average annual inflow during the study period, and monthly average storage volume. The operating periods of each reservoir and data records are heterogeneous, from 1943 to 2018 (75 years) in the case of the oldest infrastructure, and from 2012 to 2018 (6 years) for the most recent. It should be noted that inflows were estimated through a mass balance approach by the administration responsible for the management of each reservoir.

Source (3) was used to obtain the relationship between the stored volume and the flooded surface (Area Volume Elevation curve, AVE). This enabled to deduce the average monthly flooded area for each of the reservoirs during the study period.

Finally, from source (4), daily records of meteorological data were obtained from 94 automatic stations for the subsequent processing (maximum and minimum temperature and relative humidity, wind speed and solar radiation). In this case, the study period comprised 21 hydrological years (October 2000 to September 2021). From these data, the evaporation rate of each reservoir was estimated using three different methods (Hargreaves, Penman, and FAO Penman-Monteith), as reported by García-López et al. (2023a). The results obtained were compared with the values provided by (Témez, 2007), which are included in the Hydrological Plans and the SIMPA (*SIMulación Precipitación-Aportación*) model, a rainfall-runoff model used by the Administration to estimate water resources at national level (Estrela and Quintas, 1996; Ruiz García, 1998). Eventually, the FAO Penman-Monteith method was selected for this study since it provided the most consistent results (Eq. 1).

$$ET_o = \frac{0.408\Delta(R_n - G) + \gamma \frac{900}{T+273} u_2 (e_s - e_a)}{\Delta + \gamma(1 + 0.34u_2)} \quad [1]$$

where ET_o is the reference evapotranspiration (mm day^{-1}), γ is psychrometric constant (kPa $°C^{-1}$), u_2 is wind speed at 2 m height (m s^{-1}), e_s is saturation vapour pressure (kPa), e_a is actual vapour pressure (kPa), Δ is slope vapour pressure curve (kPa $°C^{-1}$), R_n is net radiation

Table 2
Extension of Andalusian hydrographic demarcations.

Hydrographic Basin	Total Surface (km^2)	Surface in Andalusian territory (km^2)	% Basin surface in Andalusia	Fraction of Andalusia (%)
Guadalquivir*	57,073	51,486	90.2	58.8
Andalusian Mediterranean	17,964	17,964	100.0	20.5
Tinto, Odiel, Piedras	4744	4744	100.0	5.4
Guadalete-Barbate	5978	5978	100.0	6.8
Guadiana*	55,528	5613	10.1	6.4
Segura*	18,880	1819	9.6	2.1
Total	160,166	87,604		100.0

* Intercommunity basins

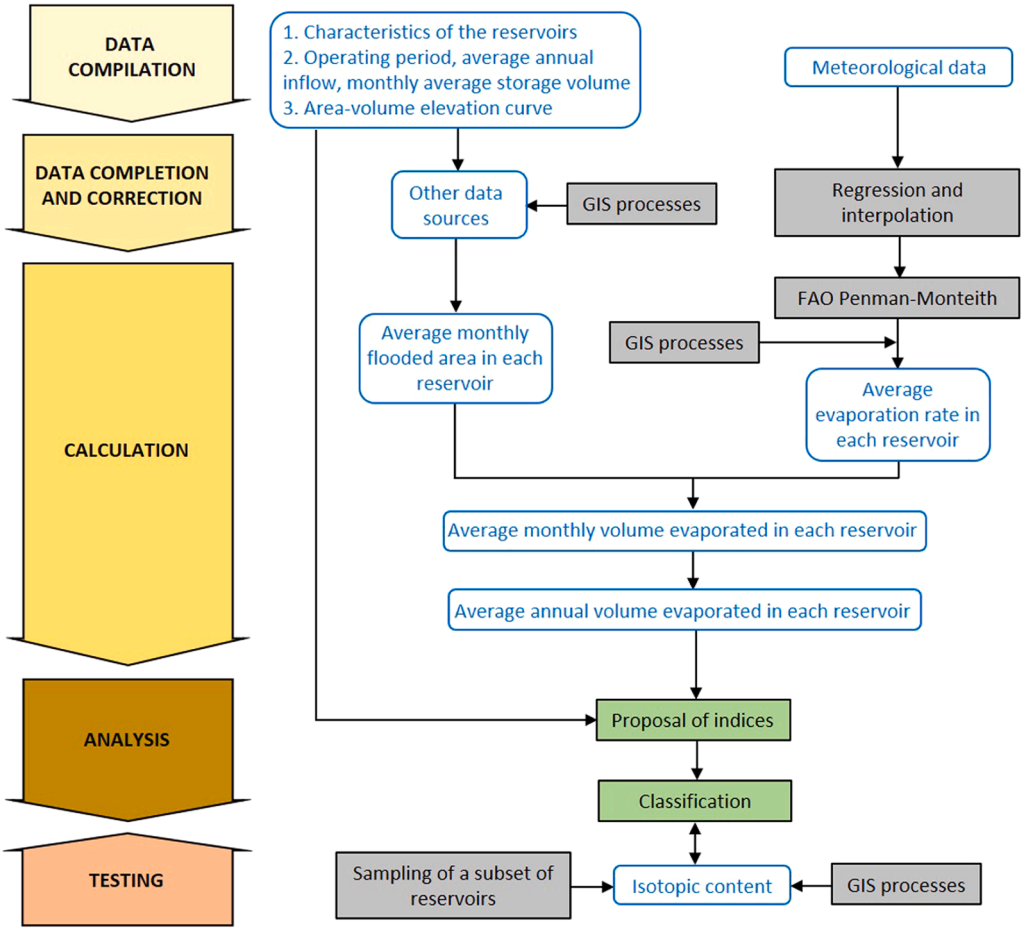

Fig. 2. Flowchart of the methodology followed in this research.

(MJ m^{-2} day^{-1}), T mean daily air temperature (°C) and G is ground heat flux (MJ m^{-2} day^{-1}).

Once created, the database was corrected to eliminate errors and fill data gaps. Three main obstacles were encountered in this stage: (i) Data on annual mean inflows during the operative life of the infrastructures was not available for nine reservoirs, so this information had to be retrieved from the SIMPA model, considering the average annual inflows for a 25 year-period; (ii) Likewise, these same nine reservoirs lacked data on the monthly average stored volumes. This limitation was overcome by using an alternative source of information (www.embalses.net) that provides graphical representations of the monthly average storage over the last 10 years; and (iii) In 4 reservoirs, the information sources did not provided data on the volume-flooded area ratio, so it had to be estimated through GIS procedures using a digital terrain model (resolution 5x5m).

Subsequently, since the available data on the ratio "stored volume/flooded area" for each reservoir corresponds to data pairs obtained at regular stage intervals (between four and seven pairs of data), it was necessary to adjust a mathematical function that expressed this relationship (through the least square method). This enabled to calculate the flooded surface for a given stored volume. Finally, the monthly average volume evaporated (in m^3) from each reservoir was estimated as the product of the monthly average evaporation rate (in mm × 0.001) by the monthly average flooded area (in m^2) and by aggregation, the annual volume evaporated. The mathematical expression is given in Eq. [2].

$$V_E = \sum_{i=1}^{12} (R_i \cdot \overline{A}_i) \quad [2]$$

where V_E Annual evaporated volume for a given reservoir (m^3)

R_i Evaporation rate in the month "i" (mm)

$\overline{A}_i$ Mean flooded area in the month "i" (m^2)

and $\overline{A}_i = f(\overline{V}_i)$ where f is the adjustment function between variables A and V

$\overline{V}_i$ Average stored volume in the month "i" during the service life

Once calculated, the results of average annual evaporation in each reservoir were compared with several variables (depth, inflows, stored volume, elevation). Such comparison evidenced substantial differences that could not be justified solely by the size of the

reservoir. This has led to the proposal of a method for classifying the efficiency of reservoirs with respect to evaporation based on the use of two indices that were calculated from hydrological parameters as explained below. Both indices, designates "Storage efficiency with respect to the evaporation (I_1)" and "Supply efficiency with respect to the evaporation (I_2)", are defined in the range between 0 and 1 and are calculated using Eq. [3] and Eq. [4]:

$$I_1 = \frac{\sum_{i=1}^{n} \left(\frac{V_{s,i} - V_{e,i}}{V_{s,i}} \right)}{n} \quad [3]$$

$$I_2 = \frac{\sum_{i=1}^{n} \left(\frac{V_{i,i} - V_{e,i}}{V_{i,i}} \right)}{n} \quad [4]$$

where I_1: Storage efficiency with respect to evaporation (dimensionless)

I_2: Supply efficiency with respect to evaporation (dimensionless)

V_s: Stored Volume (mean in a year) (hm^3)

V_e: Evaporated Volume in a year (hm^3)

V_i: Inflow Volume in a year (hm^3)

i: Each year during service life or registration period

n: Number of years in the record period

The first index (I_1) expresses the relative reduction in the volume stored in the reservoir over a given period. In this case, the inclusion of the influence of the size of the infrastructure enables to compare reservoirs of very different dimensions. Whereas reservoirs with very small losses to atmosphere will have an I_1 value very close to 1, the reservoirs with large losses compared to the stored volume, will present values far from 1.

The second index (I_2) expresses the relative reduction in available water resources as a result of evaporation, assuming that the inflows that enter into the reservoir and do not return to the atmosphere are always exploited either for human activities (supply, irrigation, energy), for environmental uses (maintenance of ecological flows and riparian vegetation), or transferred to another system (such is the case of reservoirs with leakage problems). It must be emphasized that, in terms of management, evaporated water can be considered an almost lost resource.

Nevertheless, despite the lack of studies addressing the influence of reservoir evaporation in the local microclimate of reservoir evaporation in the particular area of this study, recent research has advanced the understanding of atmospheric moisture recycling and its implications for local climates. Theeuwen et al. (2023) calculated the local moisture recycling rate (LMR), finding that an average of 1.7 % of evaporated moisture returns as local precipitation. The study also reveals a clear correlation between the LMR and variables such as humidity, orography, latitude, available convective potential energy, wind speed and total cloudiness. This suggests that humid regions with little wind and strong convective air currents are particularly favorable for a high LMR. Zhao et al. (2021) investigated how reservoir characteristic factors (RCFs) influence local climate near reservoirs. They examined correlations between RCFs of selected dams and reservoirs with global meteorological variables. Main conclusions were (a) RCFs correlate negatively with evaporation but positively with precipitation; (b) dams and reservoirs can either weaken or strengthen various meteorological variables; and (c) RCFs have a stronger impact on precipitation than geographical factors, while evaporation is more sensitive to geographical influences. Tuinenburg et al. (2020) presented a high-resolution dataset of global atmospheric moisture connections, showing that approximately 70 % of land evaporation returns as precipitation over land, with significant regional variations. Collectively, these studies highlight the complex interactions between evaporation, precipitation, and human interventions in the hydrological cycle.

According to this index (I_2), reservoirs with scarce annual inflows would present values far from 1, while those reservoirs that undergo similar evaporation processes but have very large inflows, would experience a lower relative loss and their index would be closer to 1.

The simultaneous consideration of the indexes I_1 and I_2, with limit values of 0.95–0.875 respectively, allowed to classify the reservoirs into several categories that reflect the infrastructure's efficiency:

- Class I: High storage and supply efficiencies.
- Class II: High storage efficiency and medium supply efficiency.
- Class III Medium storage efficiency and high supply efficiency.
- Class IV: Medium storage and supply efficiencies.
- Class V: Medium storage efficiency and low supply efficiency.
- Class VI: Low storage efficiency and medium supply efficiency.
- Class VII: Low storage and supply efficiencies.

Complementary to the aforementioned methodology, the intensity of evaporative processes was assessed in a fraction of the reservoirs through isotopic techniques. For this purpose, a subset of 23 reservoirs located at a wide range of altitudes and under different climatic conditions were sampled and their content in stable water isotopes (^{18}O and ^{2}H) analysed. Samples were taken in October 2022, after a severe and prolonged drought in the region, at depths between 30 and 50 cm and generally less than 100 m from the dam

wall. The isotopic determinations were conducted in the Hydrogeology Center of the University of Malaga (CEHIUMA) using a laser absorption spectroscopy analyser (Picarro L-2120-I). The results are expressed as parts per thousand ($^{\circ}/_{oo}$) deviations as set by the internationally accepted standard VSMOW (Vienna Standard Mean Ocean Water) (Eq. 5):

$$\delta_{sample}(^{\circ}/oo) = 1000\left[\frac{[R_{sample} - R_{VSMOW}]}{R_{VSMOW}}\right] \quad [5]$$

where R_{sample} and R_{VSMOW} are the isotopic ratios ($\delta^{18}O/\delta^{16}O$ for oxygen-18 and $\delta^{2}H/\ \delta^{1}H$ for deuterium) of the sample and the VSMOW respectively. The analytical error is estimated as 0.1 $^{\circ}/_{oo}$ for $\delta^{18}O$ and 1 $^{\circ}/_{oo}$ for $\delta^{2}H$. The average altitude of the catchment basin of each reservoir was calculated under a GIS environment using the 5 m-resolution DTM produced by the Spanish National Geographic Institute (IGN), to relate the isotopic content with this variable.

Since the early development of isotopic techniques at the end of the 1960s, the influence of evaporation on the hydrological cycle and, particularly, on the stable isotope content of water has been unequivocal. The kinetic fractionation effects caused by evaporation are slightly greater in proportion for ^{18}O than for ^{2}H and are expressed by means of a parameter known as "deuterium excess (d-excess)", which according to Dansgaard (1964) is calculated as follows (Eq. 6):

$$d = \delta^{2}H - 8 \cdot \delta^{18}O \quad [6]$$

Where: d: deuterium excess

$\delta^{2}H$: deviation of the ^{18}O content with respect to the VSMOW standard according to Eq. 5

$\delta^{18}O$: deviation of the ^{2}H content with respect to the VSMOW standard according to Eq. 5

Deuterium excess is a second-order isotope parameter that initially depends on the relative humidity and sea surface temperature at the evaporative source and has been used worldwide to investigate the moisture sources of precipitation. Whereas rainfall of Atlantic origin displays average d-excess values of + 10 $^{\circ}/_{oo}$ (Dansgaard, 1964), precipitation from the Eastern Mediterranean shows d-excess values greater than + 25 $^{\circ}/_{oo}$ (Gat and Carmi, 1970) and up to + 20 $^{\circ}/_{oo}$ in the case of some rainfall events from Western Mediterranean (Cruz-San Julián et al., 1992).

In addition to being useful for identifying the origin of precipitation, the d-excess parameter is strongly affected by post-precipitation processes, especially by sub-cloud evaporation of raindrops as they fall, leading to the "pseudo-altitude" effect (Moser and Stichler, 1971), as well as by evaporation when water accumulates or flows over the land surface, and during the first stages of infiltration. Evaporation leads to a reduction in the d-excess with respect to their initial values (depending on the origin of the rain) and can even result in negative values owing to the differential fractionation of the molecules of both heavy isotopes.

5. Results and discussion

After data processing, considering the operation of the reservoirs throughout their service life until 2018, a global average annual stored volume of 6196 hm^3 was obtained, *i.e.*, 51 % of the maximum storage capacity of 76 large reservoirs studied. This volume corresponds to a flooded surface of 416.5 km^2, corresponding to 68 % of the surface at maximum reservoir level. Additionally, the average annual inflow for all reservoirs is estimated at 6824 hm^3/year.

As it would be expected from a typically Mediterranean climate, the monthly distribution of stored volumes displayed a marked seasonality in the set of reservoirs, with maximum storage values in spring (April-May) and minimum values in late summer and

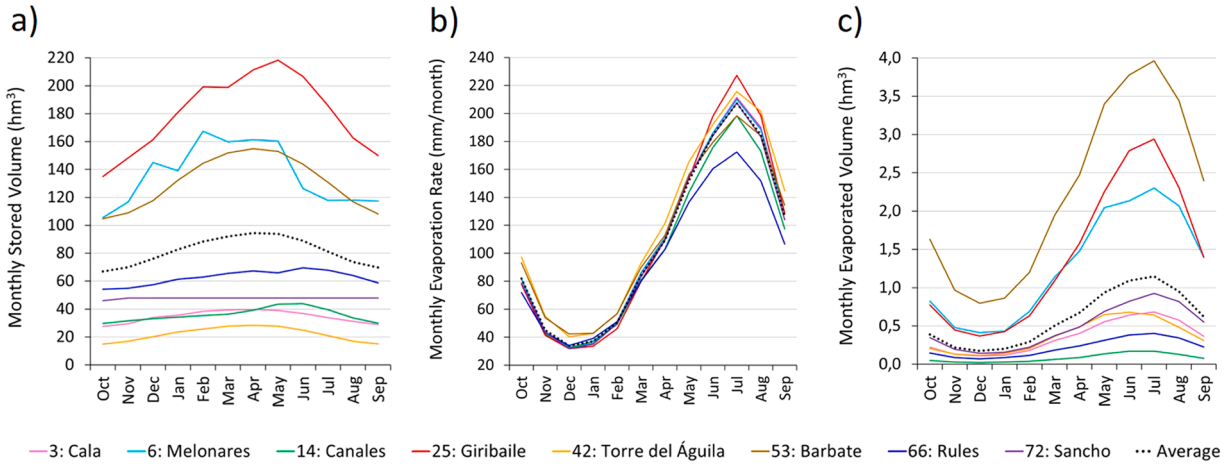

Fig. 3. Monthly distribution of a) Average volume stored during the service life, b) Average evaporation rate, and c) Average volume evaporated during the service life for a set of eight selected reservoirs (location displayed in Fig. 1). The average values of these variables for the 76 reservoirs under study are presented with the dotted line.

autumn (September-October), after the dry months. Although the general pattern is the described here, each reservoir presents a particular characteristic monthly evolution, depending on the inflow regime and the temporal distribution of the local demands. Fig. 3a shows the monthly distribution of the average volume stored in a selection of eight reservoirs during the service life of each dam, together with the average distribution for the 76 reservoirs studied (dotted line).

According to the FAO-Penman-Monteith method, the monthly evaporation rate presents minimums in December and maximums in July, with average values of 34.0 mm/month and 207.3 mm/month respectively for the set of reservoirs. The variability of the annual evaporation rate among reservoirs is between 1150 mm/year (reservoir 66: Rules) and 1426 mm/year (reservoir 42: Torre del Águila), with both values basically conditioned by the monthly average temperature and radiation. The average value for all the reservoirs studied is 1297 mm/year, with a standard deviation of 55 mm/year. Fig. 3b shows the monthly average distribution of the evaporation rate obtained for each of the eight selected reservoirs together with the average for the set of 76 dams studied.

The combination of the monthly values of the evaporation rate and the flooded area, for each reservoir, provides a first estimation of the monthly volume loss by evaporation and by, aggregation, an estimation of the average annual volume evaporated. Fig. 3c shows the monthly distribution of the average evaporated volume for each of the selected reservoirs, together with the monthly average evaporated volume in the reservoirs. The mean volume evaporated per reservoir is 7.2 hm^3/year, with a standard deviation of 7.8 hm^3/year; these values range between 0.3 hm^3/year in the reservoir that experiences less evaporation (reservoir 17: Quentar) and 34.6 hm^3/year in the reservoir suffers the highest evaporation (reservoir 52: Guadalcacín). This wide range of values is conditioned by several factors. Evidently, the size and operating regime of the reservoir determines the evaporated volume. However, for the same reservoir size there can be significant differences attributable to their morphology and, to a lesser extent, to differences in the evaporation rate. Fig. 4 shows that for the same average stored volume, evaporation losses differ greatly. For instance, for an average storage of 130 hm^3, some reservoirs lose about 8.6 hm^3/year (reservoir 24: La Fernandina), while others (reservoir 52: Barbate) triple this value (26.8 hm^3/year).

The average volume evaporated annually from the group of reservoirs is estimated at 547 hm^3/year, *i.e.*, 8.0 % of the total inflows. However, the evaporation/inflow ratio of each reservoir ranges from very low values (lower than 3 %) found in deep reservoirs from mountainous areas (*e.g.*, reservoirs 14: Canales and 17: Quentar) or in undersized reservoirs with an inflow/capacity ratio greater than 3 (reservoirs 1: Agrio, 4: Gergal and 7: La Minilla), to very high values, over 25 %, in reservoirs located in smooth orographies and with average inflows much lower than the storage capacity (reservoirs 53: Barbate, 64: La Viñuela, and 73: Piedras). In general, the greatest evaporated volumes correspond to large reservoirs such as reservoirs 52: Guadalcacín, (34.6 hm^3/year), 43: Tranco de Beas (32.1 hm^3/year) and 75: Andévalo (31.4 hm^3/year), all of them with maximum storage capacities above 500 hm^3, although with a very different operating regimes. Nevertheless, it is noteworthy the case of Barbate, a medium-large reservoir with a maximum capacity of 230 hm^3 where evaporation reaches 26.8 hm^3/year, which is attributable to its shallow bathymetry (Ruiz-Ortiz et al., 2021).

As explained in the methodology section, the consideration of the I_1 and I_2 indexes allows for a classification of the reservoirs.: Fig. 5 displays both indices in a bivariate graph and seven categories (classes) according to their supply and storage efficiency with respect to evaporation. The results of this classification are presented in Table 3.

According to this classification criterion, most reservoirs correspond to class IV, which accounts for 38.2 % of the infrastructures included in this work. This group comprises reservoirs with medium supply and storage efficiencies that are generally located in the middle course of rivers, in areas of mild topography, where evaporation causes moderate water losses annually.

The second most frequent category is class III, which accounts for 23.7 of the total. Class III includes reservoirs characterised by a medium storage efficiency but a high supply efficiency. In these infrastructures the annual inflows exceed several times the reservoir capacity and the volume lost by evaporation is relatively small.

Class V accounts for 11.8 % of the reservoirs and includes those with medium storage efficiency that, despite not being subject to extreme evaporative conditions, experiment significant water losses to the atmosphere. The reason is that the inflows in this type of

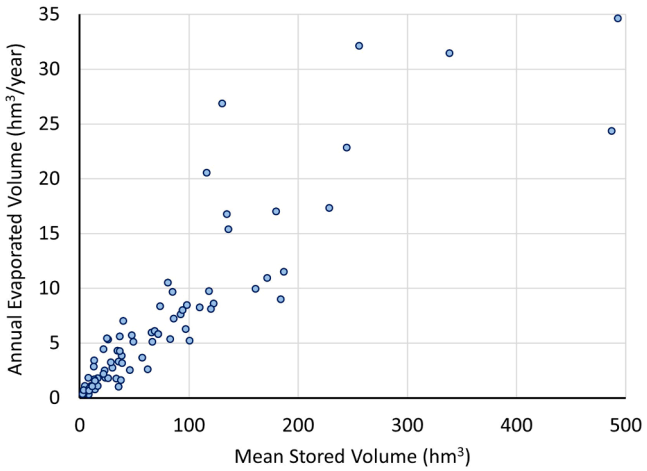

Fig. 4. Average annual volume evaporated in each reservoir *vs* the average volume stored.

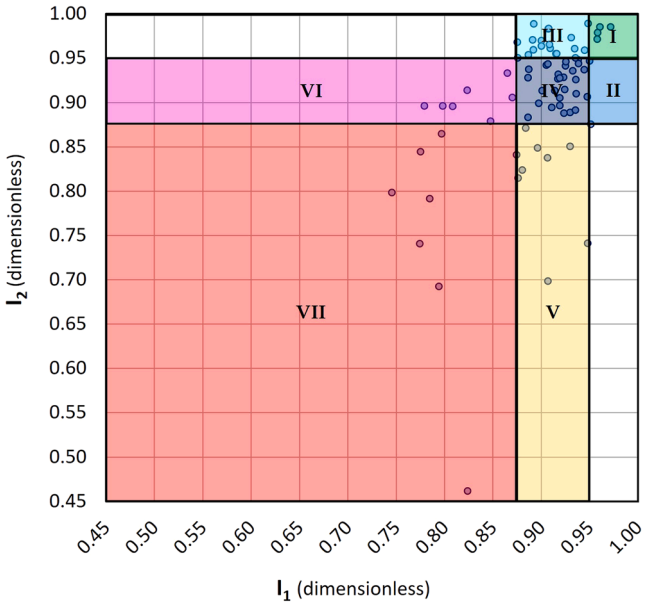

Fig. 5. Classification of Andalusian reservoirs according to their efficiency regarding evaporation.

Table 3
Classification of Andalusia reservoirs according to the methodology proposed.

Class	Storage Efficiency respect to Evaporation (I_1)	Supply Efficiency respect to Evaporation (I_2)	Number of reservoirs	Percentage of reservoirs (%)
I	0.95–1.00	0.95–1.00	4	5.3
II	0.95–1.00	0.875–0.95	2	2.6
III	0.875–0.95	0.95–1.00	18	23.7
IV	0.875–0.95	0.875–0.95	29	38.2
V	0.875–0.95	< 0.875	9	11.8
VI	< 0.875	0.875–0.95	7	9.2
VII	< 0.875	< 0.875	7	9.2
		Total	**76**	**100**

systems are relatively low, close to the maximum reservoir volume or even lower. This category includes inter-annual regulation reservoirs where water inputs from very wet years are accumulated for their later use during dry years, which implies a sustained exposure to evaporation over time.

Both classes VI and VII account for 9.2 % of the studied reservoirs. Class VI includes reservoirs with low storage efficiency and medium supply efficiency due to their relatively high annual inflows, whereas class VII comprises reservoirs that undergo very intense evaporation with respect to their average stored volume and the received inflows. This latter category includes infrastructures which design and/or operation should be re-examined as the magnitude of the evaporative losses may outweigh the benefits brought by the reservoir, thus not justifying the hydrodynamic and environmental impacts they cause in the (regulated) rivers. This aspect is especially relevant in shallow reservoirs from relatively arid areas.

Finally, classes I and II include 5.3 % and 2.6 % of the reservoirs, respectively. On the one hand, class I are infrastructures with a high storage efficiency in low evaporation contexts, typical of headwater reservoirs. These types of reservoirs are in deep valleys from mountainous areas, with low evaporation rates and usually present a favourable morphology, with considerable depths and relatively small surfaces. On the other hand, the reservoirs that fall into class II are close to the limit of class IV.

Given the uncertainty inherent to this type of estimates and the great difficulty in its quantification, the results obtained in this work have been assessed through natural tracing techniques. For this purpose, 23 reservoirs were selected and sampled once, as it was explained in Section 3.

Fig. 6a displays the relationship between the ^{18}O content and mean catchment altitude for each reservoir. The adjustment of the regression line is good, with an R^2= 0.89 and an altitudinal isotopic gradient of 0.56 $^{\circ}/_{oo}$ (per 100 m), which is mainly justified by the decrease in temperature and evaporation with altitude.

The altitudinal gradient found in the present study practically doubles that reported by several authors in groundwater samples from different locations in the southern Iberian Peninsula, *e.g.*: 0.28 $^{\circ}/_{oo}$ per 100 m in the E coastal carbonate mountain ranges of Andalusia (Benavente et al., 1990) or 0.29 $^{\circ}/_{oo}$ per 100 m in several large carbonate aquifers from Andalusia (Yanes and Moral, 2022). It is also notably higher than the values obtained in rainfall in several studies conducted in SE Iberian Peninsula: 0.27 $^{\circ}/_{oo}$ per 100 m

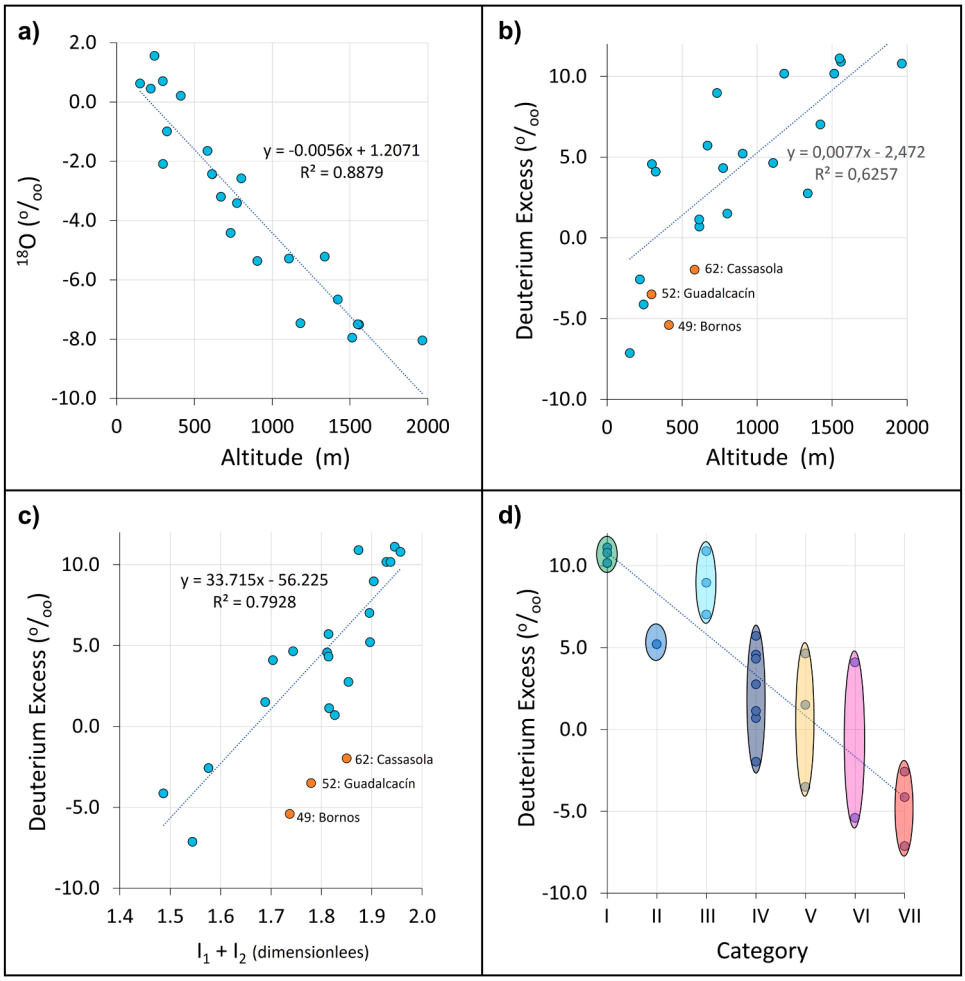

Fig. 6. Isotopic results from the set of 23 reservoirs selected. (a) Relationship between ^{18}O and altitude, (b) Relationship between d-excess and altitude, (c) relationship between d-excess and the sum of the evaporation efficiency indices (I_1+I_2) and, (d) clusters of d-excess values found in the reservoirs according to the classification proposed in this work.

(García-López, 1996), 0.19 °/oo per 100 m (Vallejos et al., 2015), and even higher than the gradient reported from specific precipitation events subject to strong evaporation: 0.40 °/oo per 100 m (García-López et al., 2023b).

This steeper gradient can be interpreted because of the reservoir's greater exposure to evaporation compared to groundwater and precipitation. While groundwater only undergoes evaporation in the early stages of deep infiltration, which occurs mainly during the winter recharge period, reservoir water is relatively stagnant and subject to intense evaporation throughout the year, especially in the summer months, when the environment is more arid (high temperatures, solar radiation, and very low air humidity). Such aridity is also conditioned by altitude, as reservoirs at lower elevations may display ^{18}O contents close to 0 or even positive, being therefore enriched in the heavy isotope with respect to the sea and showing very different values from the rain that replenishes the impoundment.

When examining the relationship between d-excess and altitude in the reservoir samples (Fig. 6b), the significant influence of altitude on this parameter is still evident, despite the somewhat greater dispersion. In the reservoirs with catchments at elevations of 1500–2000 m, the d-excess is slightly higher than 10 °/oo, a value characteristic of rainfall originated in the Atlantic, which is the main source of clouds for the area under study. Conversely, the reservoirs located at altitudes below 500 m can even show negative d-excess values. In this case, the linear adjustment is notably worse than in the case of ^{18}O, with $R^2 = 0.63$, which is attributable to the different behaviour of each reservoir regarding evaporation. For the same altitude, the difference in d-excess between reservoirs can exceed 10 °/oo. However, when d-excess is plotted against the sum of the efficiency indices proposed in this work ($I_1 + I_2$), the trend line offers a better adjustment with $R^2 = 0.79$, indicating a closer relationship between both variables (Fig. 6c). It should be noted that samples from three reservoirs were excluded from the adjustment because, due to their characteristics and operation, they presented d-excess values much lower than expected, indicating extreme evaporation. This was the case of reservoirs 52: Guadalcacín and 49: Bornos, medium-large reservoirs located in a sector highly affected by the drought at the time of the sampling campaigns. The third reservoir excluded was 62: Cassasola, a small-sized reservoir (maximum capacity 23 hm^3) highly conditioned by its operation regime. Finally,

Fig. 6d shows the reservoirs grouped according to the evaporation efficiency classes and d-excess contents. As depicted, the most efficient reservoirs with respect to evaporation are those with d-excess values over 10 $^{\circ}/_{oo}$, while the least efficient are those with values below 0. Between these two extremes, the different classes are ordered very consistently. These findings corroborate the calculations conducted in our analysis, with a good agreement between the isotopic observations and the estimates of evaporated volumes, thus lending credence to the proposed indices.

The analysis here presented can be considered a preliminary approximation because the representativeness of the isotopic data is critically influenced by the homogeneity of the water body and the sampling conditions (Rozanski et al., 2001). Besides, the annual or interannual regulation reservoirs in catchments affected by intense droughts can show significant fluctuations in their isotopic signature due to differences in residence time and evaporation exposure period. The internal dynamics and nature of each reservoir (*e.g.*, monomictic, dimictic, or polymictic regimes), affects the thermal stratification and mixing of the water column, thus having a direct influence on the isotopic contents and the interpretation of the d-excess parameter.

6. Conclusions

This work presents an integrative methodology to quantify evaporation from reservoirs leveraging institutional data source to estimate monthly evaporation volumes in each infrastructure and develop a combined efficiency index for their classification. Moreover, the results have been contrasted with the isotopic content (^{18}O and ^{2}H) of some of the reservoirs studied.

The methodology was applied to 76 large dams in Andalusia, a mediterranean region, and enabled to quantify the average monthly and, by aggregation, the annual volume evaporated in each reservoir. The average volume evaporated from the 76 reservoirs if of 547 hm^3/year, representing the 8.0 % of the inflows. The annual evaporation of each reservoir is mainly conditioned by morphological aspects, especially the ratio between flooded area and stored volume, the evaporation rate, and the operation regime of the reservoirs. However, notable differences between reservoirs can be identified; while the most efficient infrastructures only lose 1.1 % of their inflows, the most severely affected reservoirs show evaporative losses that exceed 30 % of the inflows, and even 50 % in the most extreme case. In the latter, the alteration of the river's natural regime might outweigh the benefits obtained from the intervention, bringing into question the selection of the construction site and usefulness of the infrastructure in certain contexts. This problem would be exacerbated by the foreseeable increase in temperature and evaporation linked to climate change.

For the purpose of comparing and classifying reservoirs regarding evaporation, two indices each ranging between 0 and 1 have been proposed: the storage efficiency index (I_1), and the supply efficiency index (I_2). These indices allowed to differentiate between high-efficiency ($I>0.95$), medium-efficiency ($0.875 <I<0.95$) and low-efficiency reservoirs ($I<0.875$) in terms of storage and supply. When combined, both indices lead to the classification of the reservoirs into seven categories. According to this classification criterion, 9 % of the reservoirs in Andalusia fall into the low efficiency category in terms of storage and supply, while only 5 % have an excellent performance regarding evaporative losses. The results have been preliminarily validated in a selection of reservoirs by analyzing the isotopic content of ^{18}O and ^{2}H and, particularly, the d-excess parameter. The isotopic analysis supports the observed differences of these reservoirs in terms of evaporation.

The authors are confident that the framework developed here will be useful for evaluating and optimizing the use of water resources, through a better understanding of reservoir's performance with respect to evaporation. This will enable to improve the reservoirs operation while minimizing water losses. Besides, this approach is expected to aid in the future design of more efficient infrastructures and water resources projects. This is particularly important considering the foreseeable context of climate change and increased water demand, an especial concern in water stressed regions.

CRediT authorship contribution statement

García-López, S.: Writing – review & editing, Writing – original draft, Supervision, Methodology, Formal analysis, Data curation, Conceptualization. **Salazar-Rojas, M.**: Writing – review & editing, Writing – original draft, Visualization, Validation, Software, Methodology, Formal analysis, Data curation. **Vélez-Nicolás, M.**: Writing – review & editing, Writing – original draft, Validation, Methodology, Formal analysis, Data curation. **Isidoro, Jorge M.G.P.**: Writing – review & editing, Formal analysis. **Ruiz-Ortiz, V.**: Writing – review & editing, Writing – original draft, Validation, Supervision, Methodology, Formal analysis, Conceptualization.

Statements & declarations

Ethical approval

Not applicable.

Consent to participate

All authors consented to participate.

Consent to publish

All authors consented to publish.

Funding

The open access fee was co-funded by Plan Propio-UCA 2025-2027 and the QUALIFICA Project (QUAL21-0019, Junta de Andalucía). This research was funded by the research group RNM373-Geociencias-UCA of Junta de Andalucía and Department of Earth Sciences of University of Cadiz. Jorge Isidoro acknowledges the support of the Portuguese Fundação para a Ciência e Tecnologia (FCT), through the strategic project UIDB/00350/2020 granted to CIMA (https://doi.org/10.54499/UIDB/00350/2020), and the strategic project LA/P/0069/2020 granted to ARNET (https://doi.org/10.54499/LA/P/0069/2020).

Declaration of Competing Interest

The authors do not declare any competing interest.

Data availability

Data will be made available on request.

References

Alazard, M., Leduc, C., Travi, Y., Boulet, G., Ben Salem, A., 2015. Estimating evaporation in semi-arid areas facing data scarcity: example of the El Haouareb dam (Merguellil catchment, Central Tunisia). J. Hydrol.: Reg. Stud. 3, 265–284. https://doi.org/10.1016/j.ejrh.2014.11.007.

Allen, G.R., Pereira, L.S., Raes, D., Smith, M., 2006. Evapotranspiración del cultivo. Guías para la determinación de los requerimientos de agua de los cultivos. Organ. óN. De. las Nac. Unidas Para. la Agric. Y. la Aliment. óN. ISBN 92-5-304219-2.

Althoff, D., Rodrigues, L.N., da Silva, D.D., Bazame, H.C., 2019. Improving methods for estimating small reservoir evaporation in the Brazilian Savanna. Agric. Water Manag. 216 (January), 105–112. https://doi.org/10.1016/j.agwat.2019.01.028.

Alvarez, V., González-Real, M.M., Baille, J., & Molina Martínez, J.M. (2007). A novel approach for estimating the pan coefficient of irrigation water reservoirs Application to South Eastern Spain. 92, 29–40. https://doi.org/10.1016/j.agwat.2007.04.011.

Aminzadeh, M., Friedrich, N., Narayanaswamy, S., Madani, K., Shokri, N., 2024. Evaporation loss from small agricultural reservoirs in a warming climate: an overlooked component of water accounting. Earth's. Future 12 (1). https://doi.org/10.1029/2023EF004050.

Aminzadeh, M., Lehmann, P., Or, D., 2018. Evaporation suppression and energy balance of water reservoirs covered with self-assembling floating elements. Hydrol. Earth Syst. Sci. 22 (7), 4015–4032.

Assouline, S., Narkis, K., Or, D., 2011. Evaporation suppression from water reservoirs: Efficiency considerations of partial covers. Water Resour. Res. 47 (7), 1–8. https://doi.org/10.1029/2010WR009889.

Benavente, J., Cardenal, J., Cruz-San Julián, J., García-López, S., Araguás, L., López-Vera, F., 1990. Content analysis of stable iso-topes in aquifers from the coastal mountainous chain of Gádor-Lújar (SE Andalusia, Spain). Memoires of the XXIInd Congress of IAH: Water Resources in Mountainous Regiones. Vol XXII, part 1, 415-424. Lausanne.

Bozorgi, A., Bozorg-Haddad, O., Sima, S., Loáiciga, H.A., 2020. Comparison of methods to calculate evaporation from reservoirs. Int. J. River Basin Manag. 18 (1), 1–12. https://doi.org/10.1080/15715124.2018.1546729.

CEDEX (Centro de Estudios y Experimentación de Obras Públicas) Gauging yearbooks. (2018) Available at: ⟨http://ceh-flumen64.cedex.es/anuarioaforos/afo/embalse-nombre.asp⟩).

CMAOT - Consejería de Medio Ambiente y Ordenación del Territorio, Junta de Andalucía. (2014). Red de Información Ambiental de Andalucía (REDIAM). Available at: ⟨https://portalrediam.cica.es/VisorRediam/⟩.

Craig I., Green A., Scobie M. and Schmidt E. (2005). Controlling Evaporation Loss from Water Storages. National Centre for Engineering in Agriculture Publication 1000580/1, USQ, Toowoomba.

Cruz-San Julián, J., Araguás, L., Rozanski, K., Benavente, J., Cardenal, J., Hidalgo, M.C., García-López, S., Martínez-Garrido, J.C., Moral, F., Olías, M., 1992. Sources of precipitation over south eastern Spain and groundwater recharge, 1992, 44B, 226.236 Isot. Study Tellus. https://doi.org/10.3402/tellusb.v44i3.15445.

Da Costa, E.M.B., Lucio, P.S., Maia, A.G., 2021. Relevance of reservoir morphometry in the evaporation process: an evaporation model for semi-arid regions. Water Resour. Manag. 35 (14), 4895–4907. https://doi.org/10.1007/s11269-021-02978-1.

Dansgaard, W., 1964. Stable isotopes in precipitation. Tellus 16 (4), 436–468. https://doi.org/10.3402/tellusa.v16i4.8993.

Deepika, S., Osman, M., Kumar, M., Sandeep, H., 2020. Suppressing evaporation from surface water reservoirs: a review. J. Agric. Eng. 57 (3), 259–273.

El, W.M.K.M., Mehanna, M.A., 2019. Estimation of evaporation losses from water bodies in the Sudan and Ethiopia. Int. J. Energy Water Resour. 3 (3), 233–246. https://doi.org/10.1007/s42108-019-00031-x.

El Bilali, A., Taghi, Y., Brioue l, O., Taleb, A., Brouziyne, Y., 2022. A framework based on high-resolution imagery datasets and MCS for forecasting evaporation loss from small reservoirs in groundwater-based agriculture. Agric. Water Manag. 262 (July 2021), 107434. https://doi.org/10.1016/j.agwat.2021.107434.

El-Mahdy, M., Abbas, M., Sobhy, H., 2021. Development of mass-transfer evaporation model for Lake Nasser, Egypt (2021). J. Water Clim. Change 12 (1), 223–237. https://doi.org/10.2166/wcc.2019.116.

Estrela, T. & Quintas, L., (1996). A distributed hydrological model for water resources assessment in large basins. RIVERTECH 96. 1st International Conference on New/Emerging Concepts for Rivers. IWRA. Sep.22-26, Chicago. USA.

Finch, J.W., & Hall, R.L. (2001). Estimation of Open Water Evaporation. A Review of Methods. R&D Technical Report W6-043/TR. In Environment Agency.

Fowe, T., Karambiri, H., Paturel, J.E., Poussin, J.C., Cecchi, P., 2015. Water balance of small reservoirs in the volta basin: a case study of boura reservoir in Burkina Faso. Agric. Water Manag. 152, 99–109. https://doi.org/10.1016/j.agwat.2015.01.006.

Friedrich, K., Grossman, R.L., Huntington, J., Blanken, P.D., Lenters, J., Holman, K.L.D., Gochis, D., Livneh, B., Prairie, J., Skeie, E., Healey, N.C., Dahm, K., Pearson, C., Finnessey, T., Hook, S.J., Kowalski, T., 2018. Reservoir evaporation in the Western United States. Bull. Am. Meteorol. Soc. 99 (1), 167–187. https://doi.org/10.1175/BAMS-D-15-00224.1.

Fuentes, I., van Ogtrop, F., Vervoort, R.W., 2020. Long-term surface water trends and relationship with open water evaporation losses in the Namoi catchment, Australia. J. Hydrol. 584 (February), 124714. https://doi.org/10.1016/j.jhydrol.2020.124714.

García-López, S., 1996. Los Acuíferos Carbonatados Alpujárrides al S.E. de Sierra Nevada. Hidrodinámica, Hidroquímica, Hidrología Isotópica y Cartografía de las Aguas Subterráneas. Ph. D. Thesis, Univ. De. Granada, Granada, Spain 490.

García-López, S., Salazar-Rojas, M., Ruiz-Ortiz, V., Vélez-Nicolás, M., Pacheco, M.J., Isidoro, J.M., 2023a. Estimación de la Tasa de Evaporación desde Embalse en Andalucía. An. Del. XXX Congr. Latinoam. De. Hidr. áulica 2022 – Vol. úMen. 2 – Hidrol. ía Superf. Y. Subterr. ánea 2, 886–897.

García-López, S., Vélez-Nicolás, Salazar-Rojas, M., Ruiz-Ortiz, V., Sánchez-Bellón, A., 2023b. Isotopic and remote sensing-based characterisation of a rainfall event over Western Sierra de Gádor (Spain): implications for carbonate aquifer recharge. Water 2023 15, 4252. https://doi.org/10.3390/w15244252.

Gat, J.R., Carmi, I., 1970. Evolution of the isotopic composition of atmospheric waters in the Mediterranean Sea area. J. Geophys. Res. 75 (15), 3039–3048. https://doi.org/10.1029/JC075i015p03039.

Gianniou, S.K., Antonopoulos, V.Z., 2007. Evaporation and energy budget in Lake Vegoritis, Greece. J. Hydrol. 345 (3–4), 212–223. https://doi.org/10.1016/j.jhydrol.2007.08.007.
Gökbulak, F., Özhan, S., 2006. Water loss through evaporation from water surfaces of lakes and reservoirs in Turkey. Eur. Water Manag. Online 03, 1–6.
Gorjizade, A., Akhondali, A.M., Zarei, H., Kaboli, H.S., 2014. Evaluation of eight evaporation estimation methods in a semi-arid region (Dez reservoir, Iran). Int. J. Adv. Biol. Biomed. Res. 2 (5), 1823–1836.
Guerschman, J.P., Van Dijk, A.I.J.M., Mattersdorf, G., Beringer, J., Hutley, L.B., Leuning, R., Pipunic, R.C., Sherman, B.S., 2009. Scaling of potential evapotranspiration with MODIS data reproduces flux observations and catchment water balance observations across Australia. J. Hydrol. 369 (1–2), 107–119. https://doi.org/10.1016/j.jhydrol.2009.02.013.
Han, K., Shi, K., Yan, X., 2020. Evaporation loss and energy balance of agricultural reservoirs covered with counterweighted spheres in arid region. Agric. Water Manag. 238 (311), 106227. https://doi.org/10.1016/j.agwat.2020.106227.
Han, K.W., Shi, K.Bin, Yan, X.J., Cheng, Y.Y., 2019. Water savings efficiency of counterweighted spheres covering a plain reservoir in an arid area. Water Resour. Manag. 33 (5), 1867–1880. https://doi.org/10.1007/s11269-019-02214-x.
Helfer, F., Zhang, H., Lemckert, C., 2011. Modelling of lake mixing induced by air-bubble plumes and the effects on evaporation. J. Hydrol. 406 (3–4), 182–198. https://doi.org/10.1016/j.jhydrol.2011.06.020.
Huang, C., Chen, Y., Zhang, S., Wu, J., 2018. Detecting, extracting, and monitoring surface water from space using optical sensors: a review. Rev. Geophys. 56 (2), 333–360. https://doi.org/10.1029/2018RG000598.
Huang, J., Shi, K., Shi, X., Hao, G., Yang, Y., 2023. Arid AREAS water-piled photovoltaic prevents evaporation effects research. Water 15 (21). https://doi.org/10.3390/w15213716.
INE, Instituto Nacional de Estadística. ⟨https://www.ine.es/jaxiT3/Tabla.htm?t= 2853&L= 0⟩ (accessed: 13/02/2022).
Junta de Andalucía. Consejería de Agricultura, Ganadería, Pesca y Desarrollo Sostenible (2022a). ⟨https://www.juntadeandalucia.es/medioambiente/portal/web/guest/areas-tematicas/cambio-climatico-y-clima/⟩. (Last accessed 13/02/2022).
Junta de Andalucía. Consejería de Agricultura, Ganadería, Pesca y Desarrollo Sostenible (2022b). ⟨https://www.juntadeandalucia.es/organismos/agriculturapescaaguaydesarrollorural/areas/infraestructuras-agrarias/regadios/paginas/agenda-regadio.html⟩. (Last accessed 13/02/2022).
Kisi, O., 2007. Evapotranspiration modelling from climatic data using a neural computing technique. Hydrol. Process. 21, 1925–1934. https://doi.org/10.1002/hyp.6403.
Köppen, W. (1936) Das geographische System der Klimate, 1–44 (Gebrüder Borntraeger: Berlin, Germany).
Li, Y., Li, S., Cheng, L., Zhou, L., Chang, L., Liu, P., 2024. High spatiotemporal estimation of reservoir evaporation water loss by integrating remote-sensing data and the generalized complementary relationship. Remote Sens. 16 (8), 1320. https://doi.org/10.3390/rs16081320.
Li, Z., Zhang, X., Jiang, C., Du, T., Zeng, L., 2023. Evolutions of water surface area and evaporation loss of Three Gorges Reservoir based on Landsat images, 1982-2021. Hupo Kexue/J. Lake Sci. 35 (5), 1822–1831. https://doi.org/10.18307/2023.0544.
López Moreno, J.I., 2008. Estimación de pérdidas de agua por evaporación en embalses del Pirineo. Cuad. De. Invest. óN. Geogr. áfica 34 (0), 61. https://doi.org/10.18172/cig.1207.
Lowe, L.D., Webb, J.A., Nathan, R.J., Etchells, T., Malano, H.M., 2009. Evaporation from water supply reservoirs: an assessment of uncertainty. J. Hydrol. 376 (1–2), 261–274. https://doi.org/10.1016/j.jhydrol.2009.07.037.
Majidi, M., Alizadeh, A., Farid, A., Vazifedoust, M., 2015. Estimating evaporation from lakes and reservoirs under limited data condition in a semi-arid region. Water Resour. Manag. 29 (10), 3711–3733. https://doi.org/10.1007/s11269-015-1025-8.
Martínez Álvarez V., Molina Martínez, J.M. y Soto García, M. (2004). Estimación mediante técnicas SIG, de las pérdidas de agua por evaporación en embalses de riego en la Comunidad de Regantes del Campo de Cartagena. En: Medio Ambiente, Recursos y Riesgos Naturales: Análisis mediante Tecnología SIG y Teledetección, Vol II (Conesa García, C., Álvarez Rogel, Y. y Martínez Guevara, J.B., Edrs.), pp. 37-45, Universidad de Murcia.
Martinez-Alvarez, V., Maestre-Valero, J.F., Martin-Gorriz, B., Gallego-Elvira, B., 2010. Experimental assessment of shade-cloth covers on agricultural reservoirs for irrigation in south-eastern Spain. Span. J. Agric. Res. 8 (. 2), 122–133. https://doi.org/10.5424/sjar/201008s2-1355.
Martínez-Granados, D., Maestre-Valero, F.F., Calatrava, J., Martínez-Alvarez, V., 2011. The economic impact of water evaporation losses from water reservoirs in the Segura Basin, SE Spain. Water Resour. Manag. 25 (13), 3153–3175. https://doi.org/10.1007/s11269-011-9850-x.
Ministerio de Agricultura, Pesca, Alimentación y Medio Ambiente. (2018). Spanish Dam Inventory. Formerly available at ⟨http://www.mapama.gob.es/es/agua/temas/seguridad-de-presas-y-embalses/inventario-presas-y-embalses/⟩.
Miranda Rodrigues, C., Moreira, M., Guimarães, R.C., Potes, M., 2020. Reservoir evaporation in a Mediterranean climate: comparing direct methods in Alqueva Reservoir, Portugal. Hydrol. Earth Syst. Sci. 24 (12), 5973–5984. https://doi.org/10.5194/hess-24-5973-2020.
Moser, H., Stichler, W., 1971. Die Verwendung des Deuterium und Sauersto 18 Gehalts bei hydrologischen Untersuchungen, in English: application of deuterium and oxygen-18 content measurements in hydrological investigations. Geol. Bavarica 64, 7–35.
Nevermann, H., Aminzadeh, M., Madani, K., Shokri, N., 2024. Quantifying water evaporation from large reservoirs: implications for water management in water-stressed regions. Environ. Res. 262 (P1), 119860. https://doi.org/10.1016/j.envres.2024.119860.
Penman, H.L., 1948. Natural evaporation from open water, bare soil and grass. Proc. Roy. Soc. A 193 (1948), 120.
Pérez, P.J., Castellví, F., 2002. Análisis de la evapotranspiración a escala local y regional en Cataluña. Ingeniería Del. Agua 9 (1), 59–72.
Priestley, C.H.B., Taylor, R.J., 1972. On the assessment of surface heat flux and evaporation using large-scale parameters. Mon. Weather Rev. 100 (2), 81–92. https://doi.org/10.1175/1520-0493(1972)100< 0081:otaosh> 2.3.co;2.
Rezazadeh, A., Akbarzadeh, P., Aminzadeh, M., 2020. The effect of floating balls density on evaporation suppression of water reservoirs in the presence of surface flows. J. Hydrol. 591 (July), 125323. https://doi.org/10.1016/j.jhydrol.2020.125323.
Rosenberry, D.O., Winter, T.C., Buso, D.C., Likens, G.E., 2007. Comparison of 15 evaporation methods applied to a small mountain lake in the northeastern USA. J. Hydrol. 340 (3–4), 149–166. https://doi.org/10.1016/j.jhydrol.2007.03.018.
Rozanski, K., Froehlich, K., Mook, W.G., 2001. Environmental isotopes in the hydrological cycle. Principles and applications. Tech. Doc. Hydrol. 121. No 39 Vol. III. UNESCO-IAEA, París.
Ruiz García J.M. (1998). Desarrollo de un Modelo Hidrológico Distribuido de Simulación continua integrado con un Sistema de Información Geográfica. Tesis Doctoral. Universidad Politécnica de Valencia.
Ruiz-Ortiz, V., García-López, S., Vélez-Nicolás, M., Sánchez-Bellón, A., Contreras de Villar, A., Contreras, F., 2021. Learning from hydrological and hydrogeological problems in civil engineering. Study of reservoirs in Andalusia, Spain. Eng. Geol. 282. https://doi.org/10.1016/j.enggeo.2020.105916.
Shalaby, M.M., Nassar, I.N., Abdallah, A.M., 2021. Evaporation suppression from open water surface using various floating covers with consideration of water ecology. J. Hydrol. 598 (October 2020), 126482. https://doi.org/10.1016/j.jhydrol.2021.126482.
Singh, V.P., Xu, C.Y., 1997. Evaluation and generalization of 13 mass-transfer equations for determining free water evaporation. Hydrol. Process. 11 (3), 311–323. https://doi.org/10.1002/(sici)1099-1085(19970315)11:3< 311::aid-hyp446> 3.0.co;2-y.
Sogno, P., Klein, I., Kuenzer, C., 2022. Remote sensing of surface water dynamics in the context of global change—a review. Remote Sens. 14 (10), 1–39. https://doi.org/10.3390/rs14102475.
Témez, J.R., 2007. Consideraciones prácticas sobre la evaporación en los embalses de la España peninsular. Rev. De. Obras. Públicas No 3476, 15–22.
Theeuwen, J.J.E., Staal, A., Tuinenburg, O.A., Hamelers, B.V.M., Dekker, S.C., 2023. Local moisture recycling across the globe. Hydrol. Earth Syst. Sci. 27, 1457–1476. https://doi.org/10.5194/hess-27-1457-2023, 2023.
Tian, W., Liu, X., Wang, K., Bai, P., Liu, C., 2021. Estimation of reservoir evaporation losses for China. J. Hydrol. 596. https://doi.org/10.1016/j.jhydrol.2021.126142.
Tian, W., Liu, X., Wang, K., Bai, P., Liu, C., Liang, X., 2022. Estimation of global reservoir evaporation losses. J. Hydrol. 607 (January), 127524. https://doi.org/10.1016/j.jhydrol.2022.127524.
Tuinenburg, O.A., Theeuwen, J.J., Staal, A., 2020. High-resolution global atmospheric moisture connections from evaporation to precipitation. Earth Syst. Sci. Data 12, 3177–3188. https://doi.org/10.5194/essd-12-3177-2020.

Vallejos, A., Díaz-Puga, M.A., Sola, F., Daniele, L., Pulido-Bosch, A., 2015. Using ion and isotope characterization to delimitate a hydrogeological macrosystem. Sierra de Gádor (SE, Spain). J. Geochem. Explor. 155, 14–25. https://doi.org/10.1016/j.gexplo.2015.03.006.

Winter, T.C., Buso, D.C., Rosenberry, D.O., Likens, G.E., Sturrock, A.M., Mau, D.P., 2003. Evaporation determined by the energy-budget method for Mirror Lake, New Hampshire. Limnol. Oceanogr. 48 (3), 995–1009. https://doi.org/10.4319/lo.2003.48.3.0995.

Wurbs, R.A., Ayala, R.A., 2014. Reservoir evaporation in Texas, USA. J. Hydrol. 510, 1–9. https://doi.org/10.1016/j.jhydrol.2013.12.011.

Xia, Q., Chen, Y., Zhang, X., Ding, J., Lv, G., 2022. Identifying reservoirs and estimating evaporation losses in a large arid inland basin in Northwestern China. Remote Sens. 14 (5), 1105. https://doi.org/10.3390/rs14051105.

Yanes, J.L., Moral, F., 2022. Relief and climate influence on isotopic composition of Atlantic-Mediterranean karst spring waters (Andalusia, southern Spain). Hydrol. Process. 36. https://doi.org/10.1002/hyp.14669.

Yang, H., Kong, J., Hu, H., Du, Y., Gao, M., Chen, F., 2022. A review of remote sensing for water quality retrieval: progress and challenges. Remote Sens. 14 (8). https://doi.org/10.3390/rs14081770.

Youssef, Y.W., & Khodzinskaya, A. (2019). A Review of Evaporation Reduction Methods from Water Surfaces.pdf. https://doi.org/10.1051/e3sconf/20199705044.

Zhang, H., Gorelick, S.M., Zimba, P.V., Zhang, X., 2017. A remote sensing method for estimating regional reservoir area and evaporative loss. J. Hydrol. 555, 213–227. https://doi.org/10.1016/j.jhydrol.2017.10.007.

Zhao, G., Gao, H., Cai, X., 2020. Estimating lake temperature profile and evaporation losses by leveraging MODIS LST data. Remote Sens. Environ. 251 (August), 112104. https://doi.org/10.1016/j.rse.2020.112104.

Zhao, G., Gao, H., 2019. Estimating reservoir evaporation losses for the United States: Fusing remote sensing and modeling approaches. Remote Sens. Environ. 226 (April), 109–124. https://doi.org/10.1016/j.rse.2019.03.015.

Zhao, Yiyang, Liu, Suning, Shi, Haiyun, 2021. Impacts of dams and reservoirs on local climate change: a global perspective. Environ. Res. Lett. 16, 104043. https://doi.org/10.1088/1748-9326/ac263c.